

Supplementary Figure 1. Chx10-Cre recombination pattern in the retina.

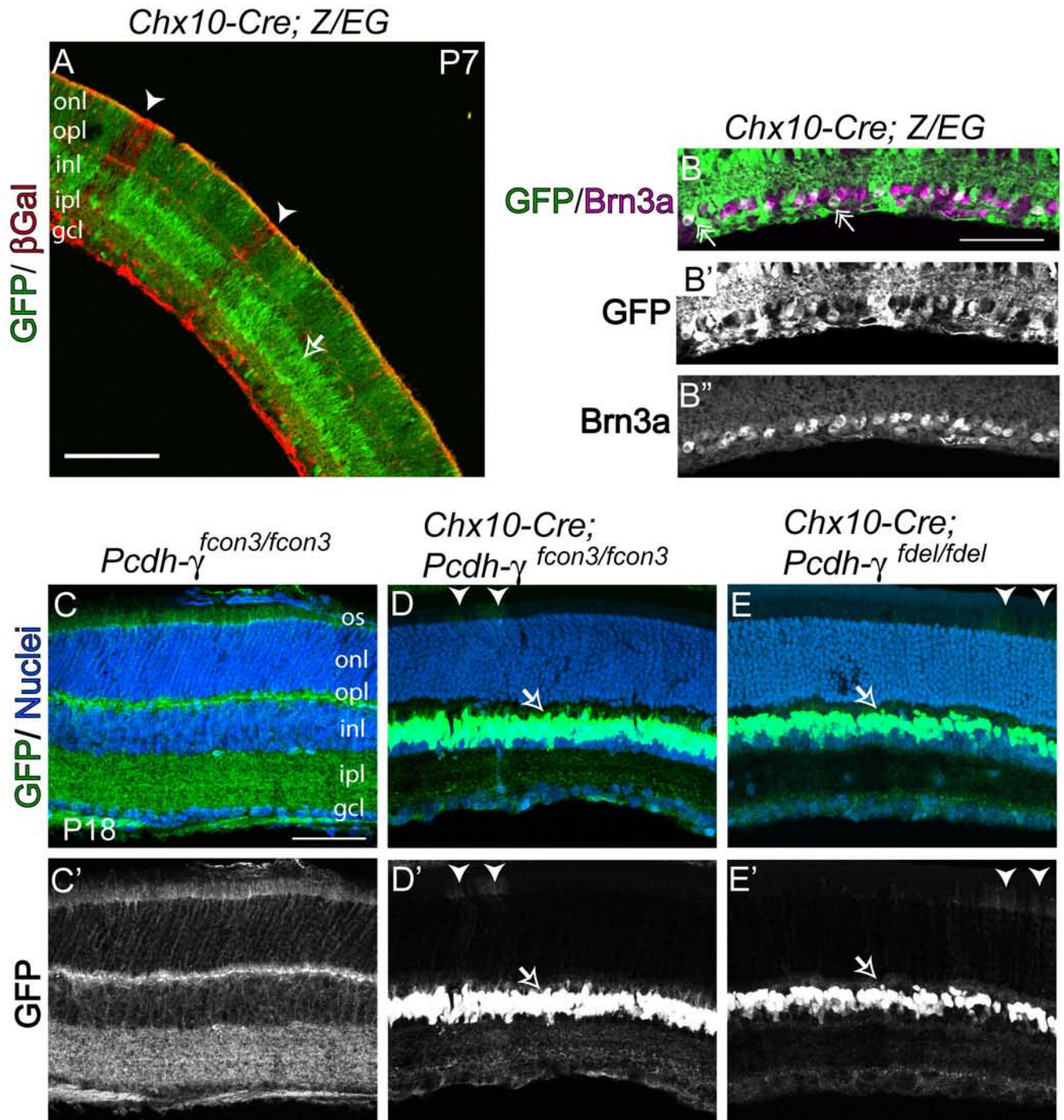
(A-B) Retina sections of *Chx10-Cre; Z/EG* P7 mice illustrate Chx10-CreGFP mediated recombination pattern, in which recombined cells express GFP (green) due to excision of the stop translation sequence in the *Z/EG* transgene. Unrecombined cells express LacZ and are immunolabeled for β -galactosidase (red). In *Chx10-Cre; Z/EG* retinas, the majority of retinal cells are descendents of progenitors that have undergone Cre-mediated recombination. However, occasional columns of cells spanning all layers and roughly half the cells present in the GCL are unrecombined (red; closed arrowhead). Chx10-CreGFP is also expressed postnatally in bipolar cells (A, D, E; green, open arrow). (B) Co-immunolabeling of *Chx10-Cre; Z/EG* retinas with GFP (green) and Brn3a (magenta) reveal that while many RGCs are spared, some RGCs are recombined (double arrow).

(C-E) Immunostaining of GFP in retina sections of *Pcdh- $\gamma^{fcon3/fcon3}$* , *Chx-10-Cre;Pcdh- $\gamma^{fcon3/fcon3}$* , and *Chx-10-Cre;Pcdh- $\gamma^{fdell/fdel}$* P18 mice report the extent of *Pcdh- γ* excision. In *Pcdh- $\gamma^{fcon3/fcon3}$* retinas, Pcdh- γ -GFP fusion proteins are present throughout the retina (C). In *Chx-10-Cre;Pcdh- $\gamma^{fcon3/fcon3}$* and *Chx-10-Cre;Pcdh- $\gamma^{fdell/fdel}$* retinas, Pcdh- γ -GFP fusion proteins are dramatically reduced, with the exception of thin stripes of GFP sparsely and variably distributed throughout the mutant retinas (detected in the outersegment and ONL; closed arrowhead). GFP in the INL reflects postnatal GFP expression of Chx10-CreGFP transgene (D, E, open arrow). Scale bar, 50 μ m.

Supplementary Figure 2. Synaptic puncta density is similar in *Pcdh-γ*; *Bax* double mutant and control retinas.

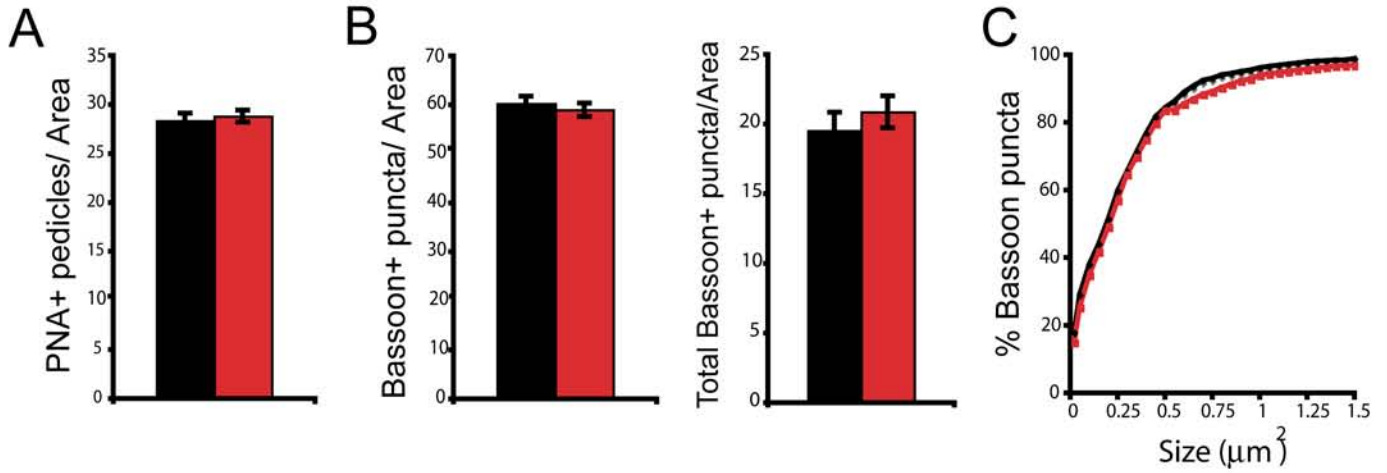
(A,B) Quantification of PNA-labeled cone pedicles and Bassoon-immunolabeled puncta in the OPL of control and *Chx10-Cre; Pcdh-γ^{fcon3/fcon3}; Bax^{-/-}* retina sections of P28 mice. Bars show mean +/- SEM of 15-18 microscope fields from three double mutant animals (red bars) and three control siblings (black bars; 2 *Chx10-Cre; Pcdh-γ^{+fcon3}; Bax^{-/-}* and 1 *Pcdh-γ^{+fcon3}; Bax^{-/-}* animals). Numbers of PNA-labeled pedicles and Bassoon-positive puncta per unit area, and total Bassoon-positive puncta area did not differ in double mutants compared to controls (by Student's t-test). (C) Cumulative histogram of Bassoon labeled puncta sizes in the OPL of double mutants compared to controls (over 900 puncta analyzed for each) shows that they did not differ in their distribution (by Kolmogorov-Smirnov test). (D) Quantification of Bassoon-immunolabeled puncta in the IPL of control and *Chx10-Cre; Pcdh-γ^{fcon3/fcon3}; Bax^{-/-}* retina sections of P28 mice. Bars show mean +/- SEM of 13-15 microscope fields at similar regions of OFF and ON lamina of the IPL of three double mutant animals and control siblings (as above). The number and total puncta area did not differ between *Pcdh-γ*; *Bax* double mutants and controls (by ANOVA). (E) Cumulative histogram of Bassoon puncta sizes in the IPL (over 3700 puncta analyzed for each) shows similar distributions in double mutants and controls (by Kolmogorov-Smirnov test).

Supplementary Figure 3. Spatio-temporal receptive fields for a sample of ganglion cells in mutant and control retinas. Each panel displays one neuron's spike-triggered average stimulus $h(x,t)$ as defined in Equation 1. Within such a receptive field, the right-most blob indicates the response polarity of the receptive field center: red for ON-cells, blue for OFF cells. In some cases (asterisks) one can see regions above and below the center with the opposite polarity. These reflect the antagonistic surround of the receptive field. For further interpretation of such receptive fields, see also (Kim et al., 2008).



Lefebvre et al, 2008.
 Supplementary Fig. 1

OPL



IPL

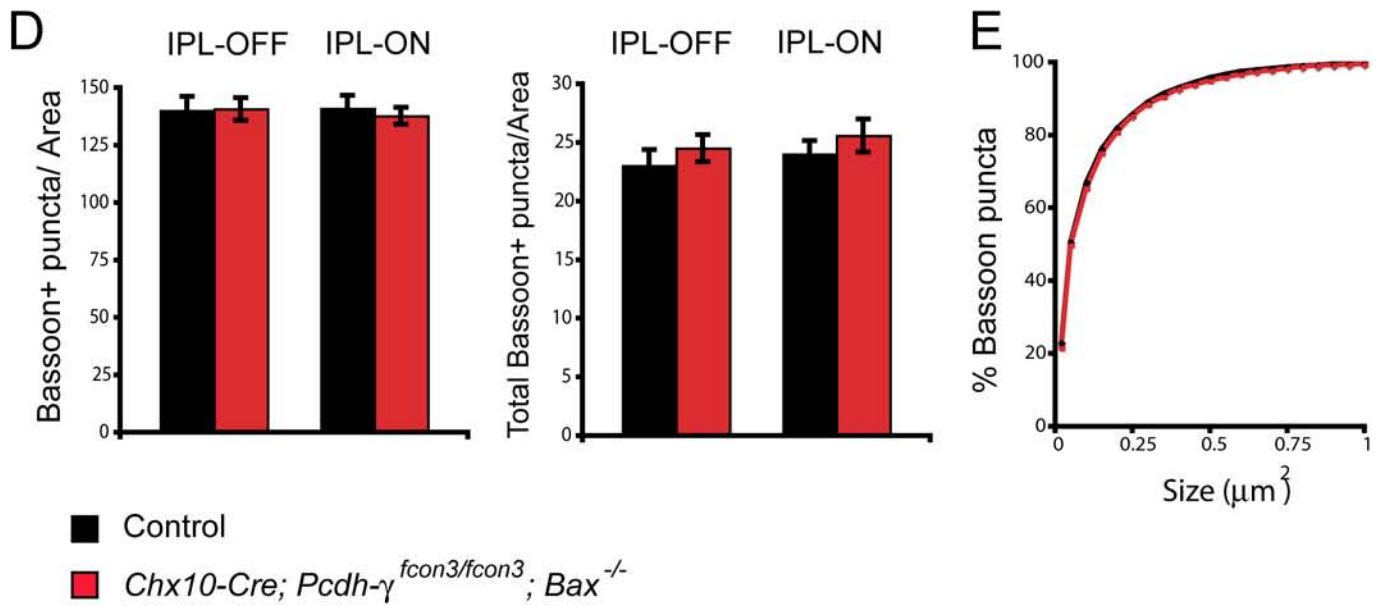
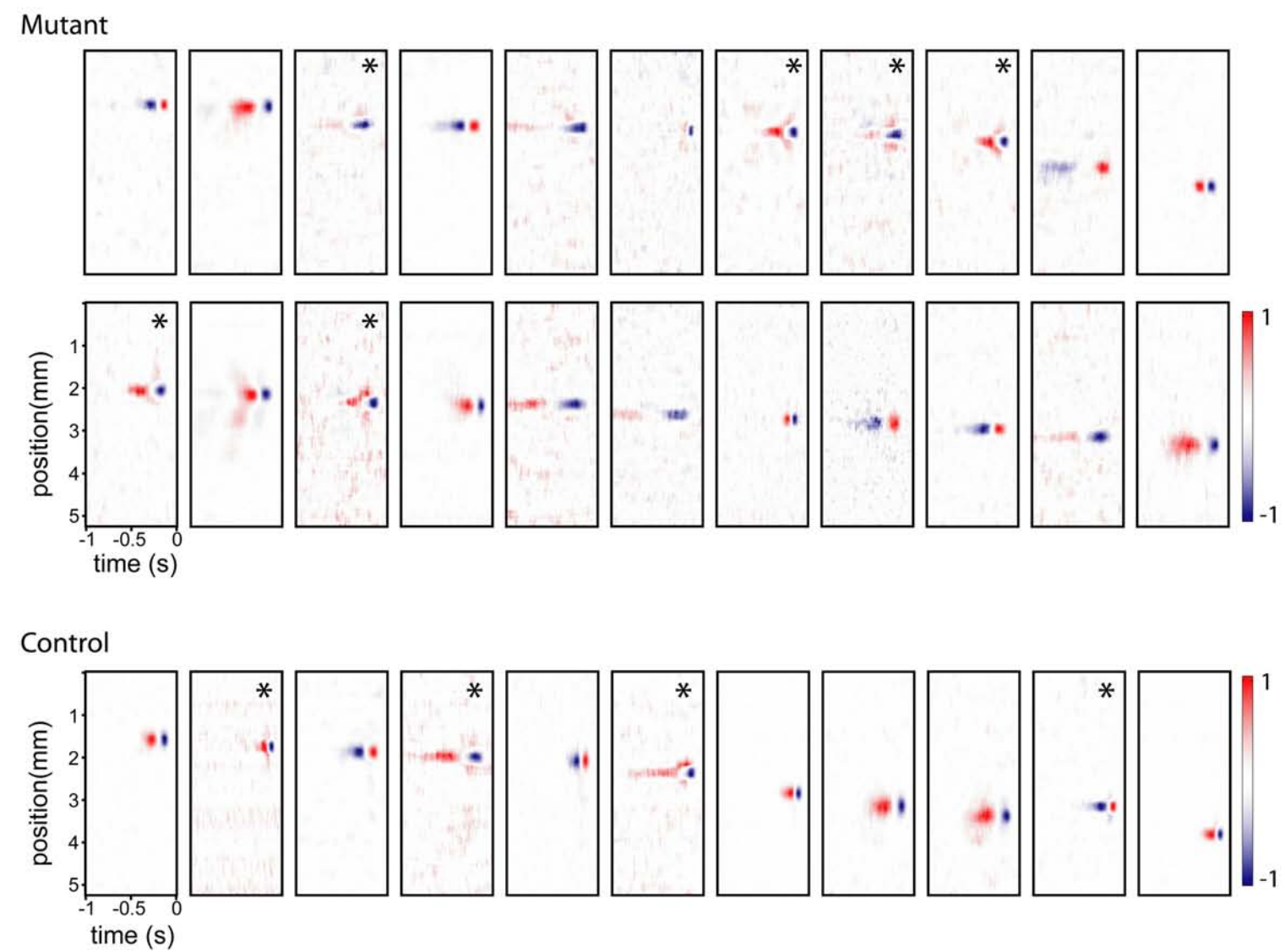


Figure S2



Lefebvre et al, 2008.
Supplementary Fig. 2

Supplementary Methods:

Synaptic puncta analysis: Retinal sections of *Chx10-Cre; Pcdh- $\gamma^{fcon3/fcon3}; Bax^{-/-}$* and *Chx10-Cre; Pcdh- $\gamma^{+fcon3}; Bax^{-/-}$* or *Pcdh- $\gamma^{+fcon3}; Bax^{-/-}$* control mice immunostained with PNA, which labels cone pedicles, or Bassoon, which labels presynaptic active zones. For PNA quantification, digital images were taken with a 40X oil immersion lens on a Zeiss LSM510 confocal microscope and PNA-labeled pedicles were quantified from a 0.05 mm² single optical section. For Bassoon puncta analysis, digital micrographs of *Pcdh- γ ; Bax* double mutant and control retinal sections were obtained at equivalent locations and laser scanning parameters with a 60X or 100x oil immersion lens on an Olympus FV1000 confocal microscope. Single optical images were processed in Photoshop, beginning with a median filter to reduce noise, and then thresholded and inverted. Puncta number, size and total puncta area within a specified unit area were determined using ImageJ software (NIH). Mean puncta number and total area were compared using ANOVA or Student's t test on condition of equivalent variances. Puncta area data was plotted as cumulative histograms, and distributions were compared using the Kolmogorov-Smirnov two-sample test.